JOURNAL OF AIRCRAFT
Vol. 44, No. 5, September–October 2007

Assessment of Ionosphere Spatial Decorrelation for Global Positioning System-Based Aircraft Landing Systems

Jiyun Lee,* Sam Pullen,† Seebany Datta-Barua,‡ and Per Enge§
Stanford University, Stanford, California 94305-4085

DOI: 10.2514/1.28199

Ground-based augmentations of the global positioning system demand guaranteed integrity to support aircraft precision approach and landing navigation. To quantitatively evaluate navigation integrity, an aircraft computes vertical and lateral protection levels as position-error bounds using the standard deviation of ionosphere spatial decorrelation. Thus, it is necessary to estimate typical ionospheric gradients for nominal days and to determine an appropriate upper bound to sufficiently cover the differential error due to the ionosphere spatial decorrelation. Both station-pair and time-step methods are used to assess the standard deviation of vertical (or zenith) ionospheric gradients (σ_{vig}). The station-pair method compares the simultaneous zenith delays from two different reference stations to a single satellite and observes the difference in delay across the known ionosphere pierce point separation. Because these ionosphere pierce point separations limit the observability of the station-pair method, the time-step method is also used to better understand ionospheric gradients at short distance scales (10–40 km). The time-step method compares the ionospheric delay of a single line of sight at one epoch with the delay for the same line of sight at another epoch a short time (a few to tens of minutes) later. This method has the advantage of removing interfrequency bias calibration errors on different satellites and receivers while possibly introducing an estimation error due to temporal ionospheric gradients. The results of this study demonstrate that typical values of σ_{vig} are on the order of 1–3 mm/km for nonstormy ionospheric conditions. As a result, σ_{vig} of 4 mm/km is conservative enough to bound ionosphere spatial decorrelation for nominal days and still leave enough margin for more active days and for non-Gaussian tail behavior.

I. Introduction

THE practicality of using the global positioning system (GPS), with ground-based augmentation, has been investigated extensively to support aircraft precision approach and landing navigation. The navigation systems greatly enhance stand-alone GPS accuracy by applying differential GPS techniques to eliminate common error sources of GPS measurements between ground stations and users. Of equal or even greater importance than improving positioning accuracy of an approaching airplane is guaranteeing flight safety by providing warnings for any system failures or anomalies and assuring the position bounds are within an acceptable level of integrity risk. The augmentations of GPS designed to fulfill these needs are the ground-based augmentation system (GBAS), such as the local area augmentation system (LAAS) being developed by the Federal Aviation Administration and the aviation industry. This paper gives detailed consideration to estimating an integrity parameter, the standard deviation of vertical ionospheric gradient, σ_{vig}, as well as bounding this value sufficiently to meet integrity requirements in the computation of protection levels.

The ionosphere, a region of charged particles in Earth's upper atmosphere (approximately 200–1500 km altitude), produces the largest range measurement errors (typically 2–10 m in the zenith direction) for stand-alone GPS standard positioning service users. For GBAS applications, almost all user ionospheric error is removed when differential corrections broadcast by nearby reference stations are applied to user measurements because the reference station sees almost the same ionospheric delay. However, residual correction errors remain due to ionosphere spatial and temporal decorrelation between reference and user. The spatial decorrelation, the larger of the two (temporal variation is negligible during transmission time), should be taken into account when the user computes protection levels (PL) which overbound the true position error [1] [the PLs are compared to alert limits (AL), the maximum allowable bounds, to determine safety of the system for each user]. This is done in the calculation of PL by using the broadcast value of a $\sigma_{\text{vertical ionosphere gradient}}$ (or σ_{vig}) parameter that expresses the typical one-sigma variation in ionospheric delay per user-to-reference separation. Thus, special care must be taken to identify the broadcast value of σ_{vig}.

Kolb et al. [2] presented a novel method to extract characteristic parameters to describe the ionosphere across local area networks of four to 50 stations with baselines of tens to hundreds of kilometers. To estimate the parameters which describe the local state of the ionosphere, an expansion of the ionospheric delay in terms of a series of orthogonal functions was used as a model and carrier-phase measurements were processed in a Kalman filter. Their work showed an estimate of 1 mm/km for σ_{vig} produced using local network data in Germany. Separately, Datta-Barua et al. [3] suggested that a typical value of σ_{vig} in the conterminous United States (CONUS) region is about 1 mm/km on nominal or "quiet" days, using ionospheric data obtained from the wide area augmentation system (WAAS) ground stations. Thus, the "typical" one-sigma gradient is already well established. However, this value is not enough to guarantee that PLs will meet aviation requirements: For a category I approach, the maximum permissible integrity risk is on the order of 10^{-7} (i.e., the PL must overbound the true position error, which is unknown in real time, with a probability of one minus 10^{-7}) [4]. The one-sigma gradient is not stringent enough for two reasons. First, the prescribed methods for the generation of PL assume a zero mean and normally distributed model for the ionosphere spatial decorrelation. However, the true ionospheric gradients are neither necessarily zero mean nor Gaussian. Second, GBAS cannot distinguish typical quiet

Received 4 October 2006; revision received 5 January 2007; accepted for publication 6 January 2007.

*Postdoctoral Researcher, Department of Aeronautics and Astronautics, Durand Building, 496 Lomita Mall.
†Senior Research Engineer, Department of Aeronautics and Astronautics, Durand Building, 496 Lomita Mall.
‡Research Assistant, Department of Aeronautics and Astronautics, Durand Building, 496 Lomita Mall.
§Professor, Department of Aeronautics and Astronautics, Durand Building, 496 Lomita Mall. Member AIAA.

conditions from "active" (but not stormy) conditions in real time. Thus, it needs to broadcast a value for σ_{vig} that bounds all such ionospheric states as opposed to only quiet conditions. Ionospheric threats under the most severe, stormy ionospheric conditions shall be detected and excluded by the GBAS ground, and such anomalous gradients are not a subject of this research.

The goal of this work is to determine the value of σ_{vig} that should be broadcast by CONUS GBAS stations. This paper fills the gap between the known one-sigma for quiet conditions and the extensive research that has been conducted to model extreme or anomalous conditions that cannot be bounded by PL without losing all system availability (e.g., see [5]). It also addresses a method of covering non-Gaussian tails of the ionospheric gradient distribution to ensure that the broadcast model always overbounds the true (unknown) distribution. This paper is organized as follows. In Sec. II, an overview of the ionosphere and its model is given. Section III explains both the "station-pair" and "time-step" methods used to estimate ionosphere spatial decorrelation. Section IV describes the two sources of postprocessed reference-station data collected from WAAS stations and continuously operating reference stations (CORS), respectively. Section V.A presents results for both estimation methods using WAAS "supertruth" data. Section V.B explains how excess noise and bias errors in postprocessed CORS station measurements are removed to the extent possible, and presents results using CORS data after noise and bias correction. In Sec. VI, σ_{vig} dependencies on geographical divisions and WAAS availability are discussed. Section VII draws conclusions with some recommendations for future work.

II. Ionosphere and Its Model

The ionosphere, located in the upper atmosphere of the Earth, is a region of gases ionized primarily by solar ultraviolet radiation. Free electrons and ions in this region affect the speed of GPS signal propagation from a satellite to a receiver. Under normal or quiet ionospheric conditions, the ionosphere delays $L1$ pseudorange measurements by several meters and advances $L1$ carrier-phase measurements by an equal amount. This amount is proportional to the total number of free electrons along the signal path, called the total electron content (TEC). The ionospheric delay I can be expressed as

$$I = \frac{K}{f^2}\int N_e \, \mathrm{d}l = \frac{K}{f^2}\mathrm{TEC} \tag{1}$$

where I is in meters, K is a constant equal to 40.3 $\mathrm{m}^3 \cdot \mathrm{s}^{-2}$, f is the carrier frequency of the signal (Hz), and the integral is of the electron density (no. of electrons/m^3) N_e, over the path length of the signal. Electron density can generally be modeled with a complicated function of height [6]. However, it is difficult to model and predict GPS impacts at the level of precision needed for GBAS applications because ionospheric activity varies with location, time of day, and time of season in addition to the 11-year solar cycle, which last peaked in 2000–2001 and will reach another peak in 2011–2012 [6]. Especially under active ionospheric conditions, such as daytime during the peak of the 11-year solar cycle, ionospheric delays can reach 30–50 m or more.

The precise estimates of ionospheric delays can be obtained using GPS measurements collected from network stations and sophisticated postprocessing algorithms (which will be explained in Sec. IV). Those delay estimates are often expressed in the "slant" domain because ionospheric delay varies with satellite elevation. The GPS signal from a low elevation satellite has a longer path in the ionosphere and thus a larger delay than one from a satellite directly overhead. Slant ionospheric delays can be converted to equivalent vertical delays using a geometric mapping function. In this work, we used the mapping function derived by approximating the ionosphere with a thin-shell model where the entire ionosphere is assumed to be a shell of finite thickness containing the condensed TEC located at 350 km above the surface of the Earth. The mapping function M or "obliquity factor," is equal to

$$M(el, h_I) = \left\{\cos\left[\sin^{-1}\left(\frac{R_e \cos(el)}{R_e + h_I}\right)\right]\right\}^{-1} \tag{2}$$

where R_e is the radius of the Earth, h_I is the height of the ionospheric shell, and el is the elevation angle of the line of sight (LOS) between a receiver and a satellite. The ionospheric obliquity factor varies from 1.0 at an elevation angle of 90 deg to just over 3.0 at that of 5 deg. By dividing a slant delay by the obliquity factor, we can convert it to the equivalent delay experienced by a user directly under the point where a LOS and the thin-shell ionosphere intersect. This point is called the ionospheric pierce point (IPP).

Ionospheric delay estimates in the "vertical" domain are used to estimate the standard deviation of ionosphere spatial decorrelation, because it must be broadcast in terms of vertical or "zenith" ionospheric delay gradients. This allows each user to multiply the vertical delay gradient by the obliquity factor to find the actual slant delay gradient for each approved satellite in view [1]. The errors introduced by this conversion are small when the ionosphere is quiet and relatively uniformly distributed. The standard deviation of vertical ionospheric gradients, σ_{vig}, is most easily expressed in terms of mm/km, although its units in the LAAS interface control document [7] are m/m. The ionospheric gradient is almost always very small (less than a few mm/km), but it can become significant (a few hundred mm/km) under active ionospheric conditions; such anomalous gradients are beyond the scope of this paper.

III. Ionospheric Gradient Estimation Method

Ionospheric spatial gradients are estimated using two methods, the station-pair and time-step methods, based on different configurations of stations and satellites. The observablility of ionospheric gradients and possible bias effects on gradient estimates are discussed for each method.

A. Station-Pair Method

The station-pair method treats each pair of stations as a GBAS ground-station and aircraft receiver pair. Pairs are configured to view the same satellite as shown in Fig. 1. Ionospheric vertical delays for each of the two stations are differenced at each epoch. The ionosphere can be approximated with the thin-shell model and the IPP is the point of intersection of this thin shell and the receiver–satellite LOS as explained earlier. Differential delays are then divided by the IPP distance between the two stations to compute vertical ionospheric gradients.

Because of the small magnitude of nominal ionospheric gradients, their estimates can be easily corrupted by any noises or biases. A typical bias is the interfrequency bias (IFB) which results from instrumental biases in both the receiver and GPS satellite transmitters caused by hardware delays in the $L1$ and $L2$ signal paths [8]. Because

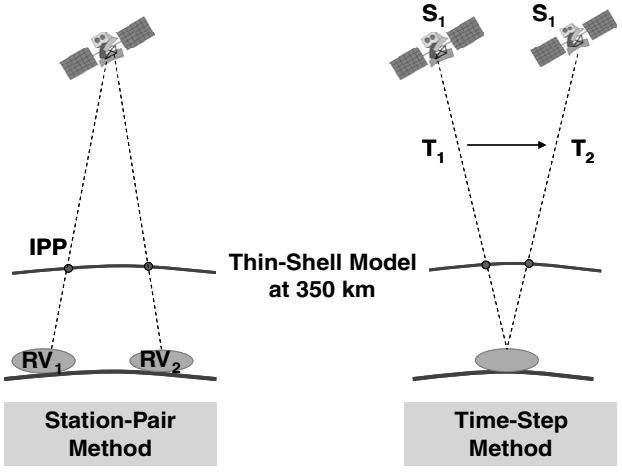

Fig. 1 Satellite and receiver configuration for the station-pair and time-step methods.

Table 1 Data set

	Geomagnetic storm class	K_P	D_{ST}	WAAS coverage
2 July 2000	N/A (quiet day)	1.7	2	Nominal ($\geq$ 99%)
11 Sept. 2002	Moderate	5.0	−78	∼95%
25 July 2004	**Strong**	**8.0**	**−148**	**∼73.7%**
26 July 2004	Strong	7.3	−94	∼96.4%
27 July 2004	Severe	8.7	−197	∼96.4%
22 Aug. 2004	**N/A (quiet day)**	**3.3**	**−37**	**∼24.7%**
9 Nov. 2004	Severe	8.7	−223	∼96%
10 Nov. 2004	Severe	8.7	−287	∼96.4%

two stations viewing the same satellite are paired in this method, the satellite IFB calibration error is canceled out when differencing the vertical delays. However, the receiver IFB calibration error may still remain. The IPP distance in the station-pair method depends on the physical separation of stations. Therefore, ionospheric measurements collected from a dense station network (e.g., the continuously operating reference stations) are adequate to measure the ionospheric gradients at short distances when used with this method.

B. Time-Step Method

The time-step method was introduced to gain sufficient sampling at distances less than the physical separation of stations [3]. This method groups a single satellite and a single receiver as a pair as shown in Fig. 1. The ionospheric delay between the satellite and receiver at one epoch (T_1) is compared with the delay for the same pair at a later epoch (T_2). The gradient is then computed by dividing the differential delay by the distance between the IPP at T_1 and the IPP at T_2. With this configuration, therefore, the spatial separation of interest (i.e., short distances of 10–40 km for the GBAS application) can be obtained by adjusting the time interval (Δt).

This approach bears less architectural resemblance to the GBAS ground-station and aircraft scenario than the station-pair configuration, and thus it may not be intuitive to connect this method to the GBAS application. Nonetheless, this configuration captures the same ionospheric effect as a ground-station receiver and an aircraft receiver whose LOS to a satellite penetrates neighboring regions of the ionosphere. When differentiating the delays of the same satellite and receiver pair, both the satellite and receiver IFB calibration errors are eliminated. However, the time-step method introduces another error source: the temporal decorrelation error. Because the delays of different epochs are used to estimate the ionosphere spatial decorrelation, the estimated gradients would be a mixture of the spatial gradient and the temporal gradient (which cannot be extracted easily from the total gradient estimates).

IV. Data

The data used to estimate nominal ionosphere spatial gradients are of two types: the WAAS postprocessed network data (known as supertruth) and data from the CORS postprocessed by the Jet Propulsion Laboratory (JPL) . CORS data are adequate for the station-pair method because of the relatively dense CORS receiver network. However, WAAS data are of higher quality since each reference station has three high-quality receivers that aid in removing measurement outliers and reducing noise.

A. WAAS Supertruth Data

The WAAS network consists of 75 WAAS reference element (WRE) receivers located at 25 reference stations (i.e., each station has three nearly colocated dual-frequency receivers). To generate high-precision ionospheric TEC data, carrier-phase measurements collected from the 75 receivers are first cleaned by identifying cycle slips. Carrier-phase-based ionospheric delay measurements (generated from carrier-phase measurements on both the $L1$ and $L2$ frequencies) are then leveled by computing the average of code–minus–carrier ionospheric observables. Using the very-precise leveled ionospheric measurements, a Kalman filter solves for instrument biases. Satellite and receiver interfrequency biases are removed from the leveled carrier-phase ionospheric observables to obtain (almost) unbiased phase-leveled ionospheric TEC observables. The corrected data sets are then passed through a voting algorithm to select one of three measurements (from three colocated receivers) as the ground "truth." The final output of this process operated by Raytheon Systems Corporation is the supertruth data: high-precision estimates of ionospheric delay.

The WAAS supertruth data are less noisy than the JPL postprocessed CORS data because of high-quality receivers and antennas with the same firmware versions and the voting scheme explained above. However, the limited number of stations results in larger separations between stations (typically at least several hundred kilometers), which makes it difficult to observe ionospheric behavior at GBAS-applicable distance scales (on the order of tens of kilometers or less).

B. JPL Postprocessed CORS Data

GPS measurements collected from a network of CORS (more than 400 stations over CONUS) are made available to the public via the U.S. National Geodetic Survey website[¶]. Using CORS data, high-precision ionospheric measurements were generated at JPL using the "truth processing" method similar to that described in Sec. IV.A. The detailed algorithm described by Komjathy et al. [9] may be summarized as follows. Raw data from the receiver independent exchange format (RINEX) files was processed using NASA's GPS-inferred positioning system (GIPSY) module Sanity Edit (SanEdit) to detect cycle slips [10]. The cycle-slip criterion was set at 18 cm, which requires the assumption that ionospheric variation is not rapid during nominal days. A tighter slip parameter would cause the editor to remove excessive data points and consequently degrade data accuracy because the accuracy of leveling depends highly on the length of continuous arcs of data [9]. The carrier-phase-based ionospheric measurements were then leveled using the code ionospheric observables and an elevation-dependent weighting function [9]. The satellite and receiver interfrequency biases were then estimated using GIPSY and the JPL's global ionosphere mapping (GIM) software and corrected to the degree possible to provide high-precision ionospheric measurements.

The noise level of JPL–CORS data is about 1 order of magnitude higher than that of WAAS supertruth data. This is mainly due to the fact that CORS receivers and antennas come in all shapes, forms, and levels of quality. However, as addressed earlier, the dense CORS network, with more than 400 stations in CONUS, allows the examination of ionospheric characteristics at smaller scales. Therefore, if the higher noise of CORS measurements can be reduced effectively (as will be discussed in Sec. V.B), CORS data may be more useful for this study than WAAS data.

C. Data Set

The analysis described in this paper was carried out using data from 8 days listed in Table 1. The data of ionospheric nominal days was chosen from the WAAS supertruth archive to include all nominal and ionospherically active days that were not classified as

[¶]Data available online at http://www.ngs.noaa.gov/CORS/download2/ [retrieved 20 August 2006].

"ionosphere storm" days. Table 1 shows the geomagnetic storm class, Kp index, Dst index, and WAAS coverage for each day. The Kp and Dst (direct) indices are measures of the magnetic perturbation of Earth's atmosphere. For example, the absolute value of the Dst index was larger than 400 during the 20 November 2003 ionospheric storm, whereas absolute values of the Dst index on nominal days are almost always below 40. The geomagnetic storm class has been defined based on Kp indices. By design, the days listed in Table 1 cover all storm classes except those which produce ionospheric gradients within the ionosphere anomaly threat model (i.e., spatial gradients greater than 30 mm/km [5]).

WAAS coverage indicates the percentage of the WAAS coverage volume in which the WAAS lateral precision with vertical guidance (LPV) service was available at least 95% of the time. This study was initially conducted on 6 days for which the WAAS coverage was better than 90%. Two more days (shaded in Table 1) were added later to examine the sensitivity of ionospheric gradients to WAAS LPV availability (details are in Sec. VI.B).

V. Results

A. Results from WAAS Supertruth Data

1. *Estimation Results Using Station-Pair Method*

Figure 2 shows the spatial decorrelation result for a quiet day (2 July 2000), which exhibited nominal ionospheric behavior, using the station-pair method and the WAAS supertruth data. The two-dimensional histogram of the number of observations is shown as a function of both the IPP separation distance and the difference in vertical ionospheric delays (dI). The horizontal axis divides the IPP separation distances into bins, the vertical axis divides observations of the difference in vertical delays into bins, and the gray scale of each pixel indicates the number of measurements counted. Although no data were available for distances less than 50 km due to physical distances between WAAS stations, a fairly smooth and linear behavior of differential ionospheric delays as a function of IPP separation was observed at distances between 100 to 1000 km. The differential delays were divided by the corresponding IPP separation distances to obtain vertical ionospheric gradients.

The distribution of normalized vertical ionospheric gradients is shown in Fig. 3 on a logarithmic scale. The vertical gradients are normalized by removing their mean and dividing them by their standard deviations (detailed steps will be given shortly). It is clearly seen that the distribution (the dotted curve) derived from the observations shown in Fig. 2 has non-Gaussian tails. Because LAAS users assume a zero-mean normally distributed error model in the computation of protection levels, the nominal sigma (1σ) of a zero-mean Gaussian distribution—shown as the dashed curve—should be inflated to cover the non-Gaussian tails of the actual distribution. The inflation factor needed for the 2 July 2000 data was 1.42. The 1.42σ Gaussian distribution (the solid curve) well overbounds the empirical distribution (the dotted curve).

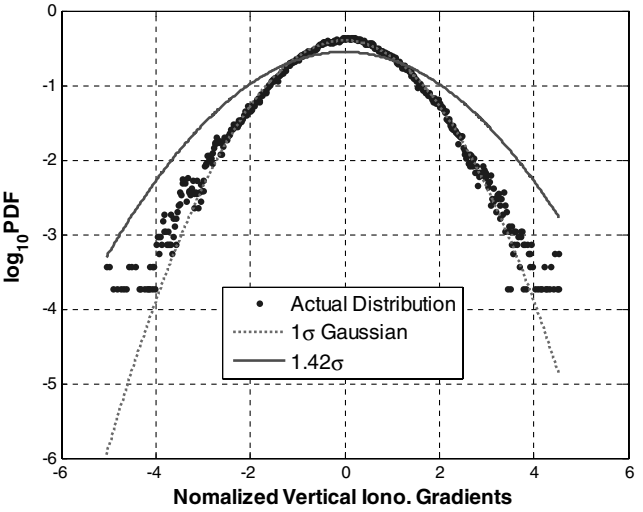

Fig. 3 Probability density function of normalized vertical ionospheric gradients on a quiet day (2 July 2000).

The sigma overbounding method is used as follows. First, vertical ionospheric gradients are divided into bins of IPP separation distance. Second, the mean (μ_{vig}) and standard deviation (σ_{vig}) of vertical ionospheric gradients in each bin are computed, interpolated at each distance corresponding to each gradient, and used to normalize the gradients. Based on the distribution of normalized ionospheric gradients, the inflation factor (f) is then determined as shown in Fig. 3. Lastly, the "σ_{vig} overbound" is computed as $|\mu_{vig}| + f\sigma_{vig}$ for each bin. Figure 4 shows the σ_{vig} overbound result for a quiet day (2 July 2000). The estimated σ_{vig} overbounds (the curve with asterisks) are less than 2 mm/km and the one-sigma values (the curve with circles) are just below 1 mm/km at distances greater than 200 km. The estimates at distances less than 200 km cannot be trusted because the number of samples is not sufficient to obtain reliable statistics of vertical ionospheric gradients. The numbers of samples per bin for distances below 200 km are less than a thousand while those per bin for distances above 200 km are on the order of tens of thousands.

The σ_{vig} overbounds were estimated for all six days listed in Table 1 using the station-pair method and the WAAS supertruth data. The results are shown in Fig. 5. The solid curves show the one-sigma

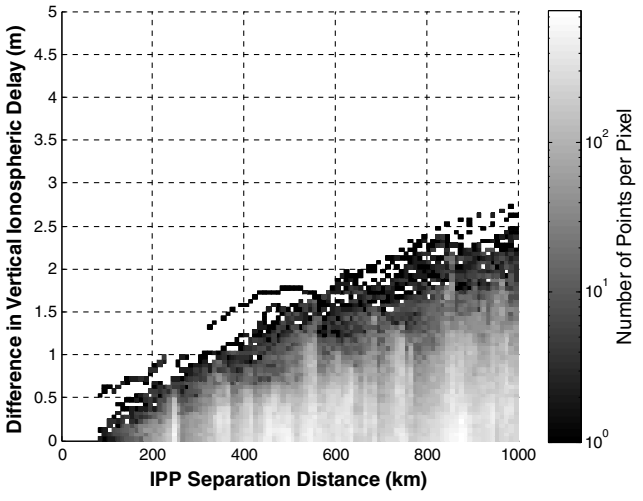

Fig. 2 Differential vertical ionospheric delay results on a quiet day (2 July 2000) from the station-pair method and WAAS supertruth data.

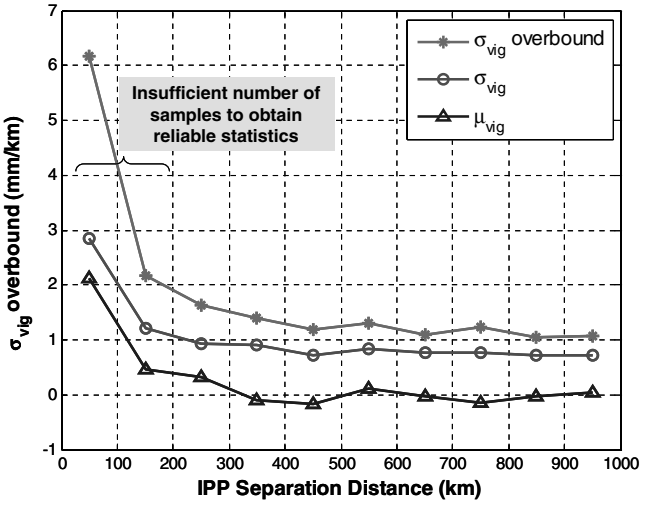

Fig. 4 σ_{vig} overbound results from the station-pair method and WAAS supertruth data for a quiet day (2 July 2000).

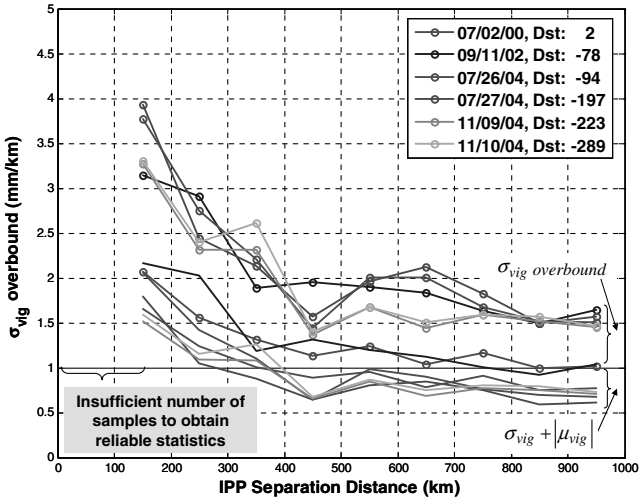

Fig. 5 σ_{vig} overbound results from the station-pair method and WAAS supertruth data for all six days.

plus the absolute value of the mean of vertical ionospheric gradients for different days. The solid line with circles shows the σ_{vig} overbound (i.e., the inflated sigma to overbound the non-Gaussian tails of the actual distribution). The inflation factors applied for each day are in the range of 1.3–2.6. The results show that the sigmas including those of severe days can be bounded by 4 mm/km. However, the station-pair method combined with the WAAS supertruth data has certain limitations when applied to the GBAS scenario. First, a reliable statistic is not available at IPP separation distances below 100 km due to the sparse network of WAAS stations. Second, the estimate increases as the distance decreases because of the remaining bias (e.g., the receiver IFB calibration error or the carrier-phase leveling error due to multipath and receiver noise). The same amount of bias divided by a shorter distance would magnify the bias effect on σ_{vig} estimates.

2. *Estimation Results Using Time-Step Method*

The results for all six days using the time-step method and the WAAS supertruth data are shown in Fig. 6. One-sigma plus the absolute value of the mean ($\sigma_{vig} + |\mu_{vig}|$) of the vertical ionospheric gradients is presented in the left plot for each day. The different markers indicate the different time intervals (Δt) used to configure the pairs for the time-step method. By adjusting the time interval, the ionospheric gradients can be estimated for targeted separation distances. As an example, Δt of 10 min was used to get σ_{vig} estimates at baselines longer than 100 km, and Δt of 1 min was chosen to observe ionospheric gradients at separation distances shorter than 40 km. The sigmas were then inflated by a factor of approximately 1.2–2.3 to overbound the thick tails of the true distributions. The right plot in Fig. 6 shows those σ_{vig} overbound results for all 6 days.

It is clear that the estimates of ionospheric gradients are obtainable at GBAS-applicable distances, 10–40 km, using the time-step method. However, several curves in the right plot exceed a σ_{vig} overbound of 4 mm/km, which is the maximum limit derived using the station-pair method (see Fig. 5). This is caused by ionospheric temporal gradients along with other remaining biases (due to phase-leveling errors on ionospheric measurements) degrading the results, especially at shorter distances. Although the time-step method provides a fairly good estimate of the ionospheric spatial gradient, we cannot fully rely on this method given that the temporal gradient is difficult to estimate and extract from the total gradients. To obtain a reliable σ_{vig} estimate, the two problems should be solved at the same time: observability at short distances and removal of remaining biases. This subject will be discussed with the use of CORS data in the following section.

B. Results from JPL Postprocessed CORS Data

1. *Noise Reduction and Bias Removal*

Although the dense network of CORS stations enables us to measure ionosphere spatial decorrelation at distances less than 100 km, the noise level of the JPL postprocessed CORS data is much higher than that of WAAS supertruth data. Therefore, some degree of noise reduction and bias removal are necessary to estimate ionospheric spatial gradients. To reduce the noise of CORS data, residuals between computed TEC from JPL's GIM software and measured TEC were used. A threshold of 20-sigma of residuals (which corresponds to about 50 TECU) was applied to eliminate extreme outliers. An elevation cutoff angle of 30 deg was also applied to exclude noisy measurements (due to multipath and receiver noise) because GIM is less accurate at modeling the ionosphere at low elevation angles. The remaining bias is also large at low elevation compared to that at high elevation because the length

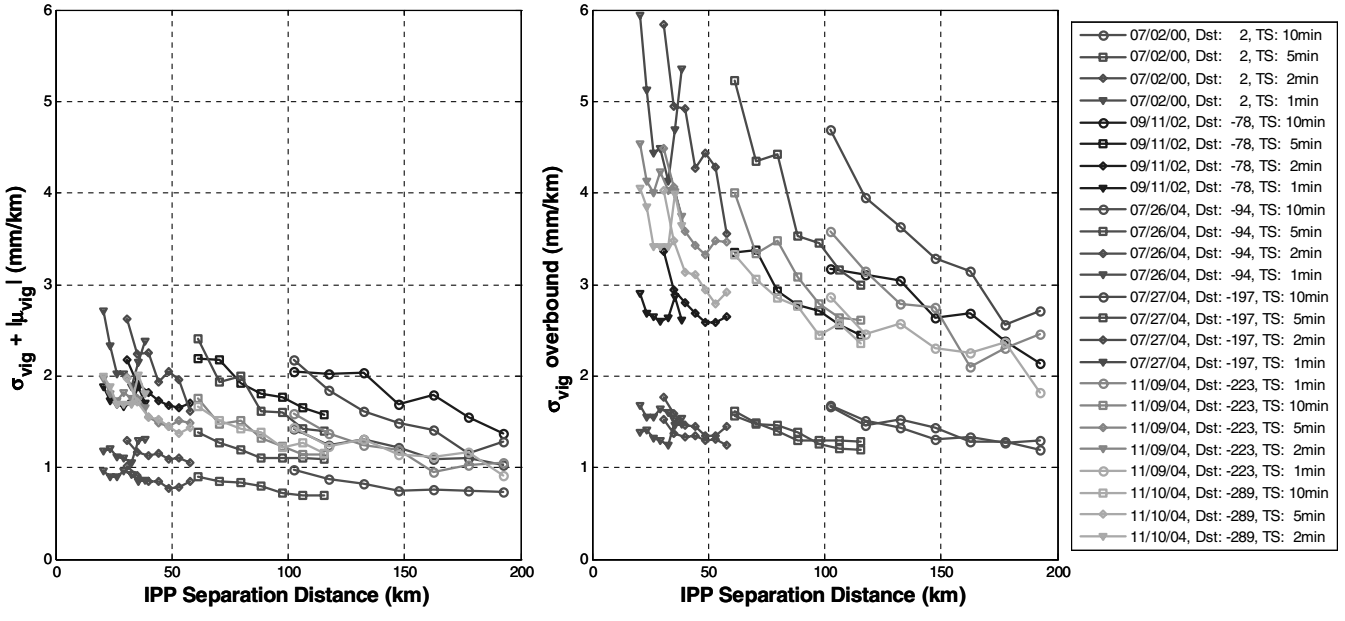

Fig. 6 σ_{vig} overbound results from the time-step method and WAAS supertruth data for all six days.

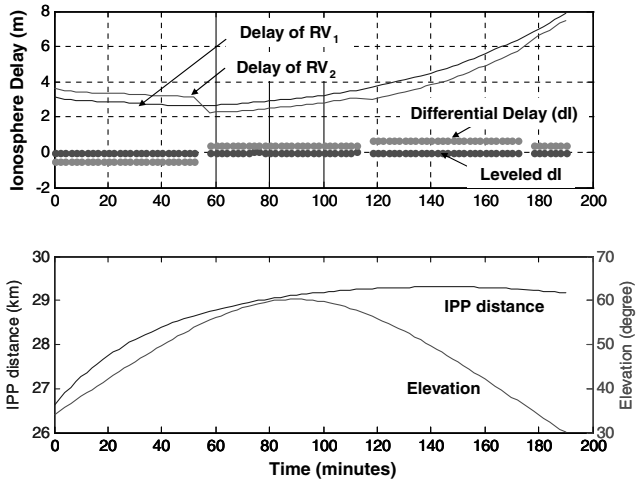

Fig. 7 Bias-removed differential ionosphere slant delays from JPL postprocessed CORS data.

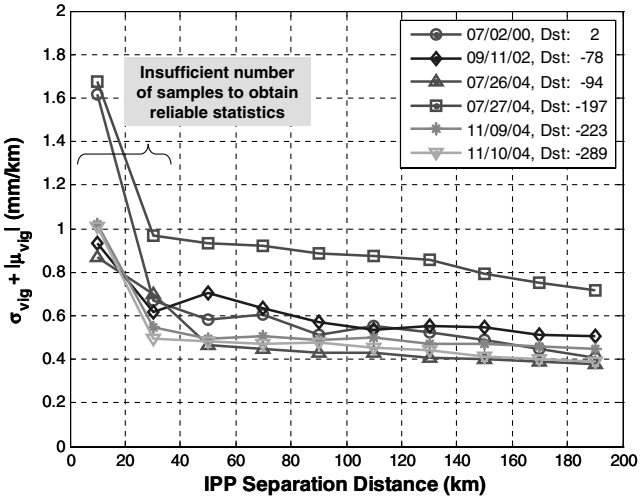

Fig. 9 $\sigma_{vig} + |\mu_{vig}|$ results from the station-pair method and JPL–CORS data for all six days (with noise reduction and bias removal).

of the continuous arc of ionospheric observables is typically shorter due to frequent cycle slips at low elevation. For short arcs, elevation weighting has almost no effect on averaging code-minus-carrier measurements and this introduces large leveling errors [9].

To remove the remaining biases including the carrier-phase leveling error and the IFB calibration error, we leveled differential ionospheric delays by computing the mean of differential ionospheric delays of continuous arcs. The continuous arcs were determined by applying the slip detection parameters of 5–30 cm depending on IPP separation distances and ionospheric activity of a given day. Figure 7 shows one example of the bias removal from CORS data. A pair of CORS stations looking at the same satellite (SV39) was chosen on a quiet day (2 July 2000). The two thin curves on the top plot show ionospheric slant delays of the pair. The IPP distance and satellite elevation angle are plotted, respectively, on the lower subfigure. The differential ionospheric delays (shown as the dotted lines) are corrupted by the different levels of biases at each continuous arc. As an example, a bias of about 90 cm exists on the third arc for which the corresponding IPP distance is approximately 30 km, and thus the bias is converted to an equivalent ionospheric gradient of 30 mm/km. Knowing that a good estimate of σ_{vig} is about 4 mm/km, this bias cannot be ignored in the estimation process. The darker dotted line shows leveled differential slant delays obtained after removing the biases. The leveled differential delays in the slant domain are converted to the vertical domain after dividing by obliquity factors in Eq. (2).

2. Estimation Results Using Station-Pair Method

After removing biases and noise as discussed above, the cleaned JPL–CORS data were used to estimate vertical ionospheric gradients. Figure 8 shows a two-dimensional histogram of observations as a function of the IPP separation distance and the differential ionospheric delay in the vertical domain for the quiet day (2 July 2000), obtained using the station-pair method. Note that a large number of samples is available at short separation distances (less then 40 km).

The JPL–CORS data of all six days listed in Table 1 except two days in bold were processed to estimate σ_{vig} overbounds. The results are shown with different markers for different days in Figs. 9 and 10. The curves in Fig. 9 show one-sigma plus the absolute value of the mean of the vertical ionospheric gradients for each day. The approach described in Sec. V.A.1 was taken to determine inflation factors covering the non-Gaussian tails of distributions. The σ_{vig} overbound curves shown in Fig. 10 were obtained by inflating σ_{vig} estimates by a factor of 2.2–4.1. Note that the inversely proportional trend (seen in Figs. 5 and 6) has been almost suppressed by removing the bias effect. The σ_{vig} overbounds are almost consistent at distances above 40 km except for one "severe" day (27 July 2004). The inverse-linear trend appears again in the region below 40 km because the bias cannot be removed perfectly and whatever remaining biases divided by very short distances must degrade the results. Knowing this fact, it is reasonable to extend the flat lines of 40 km or greater to

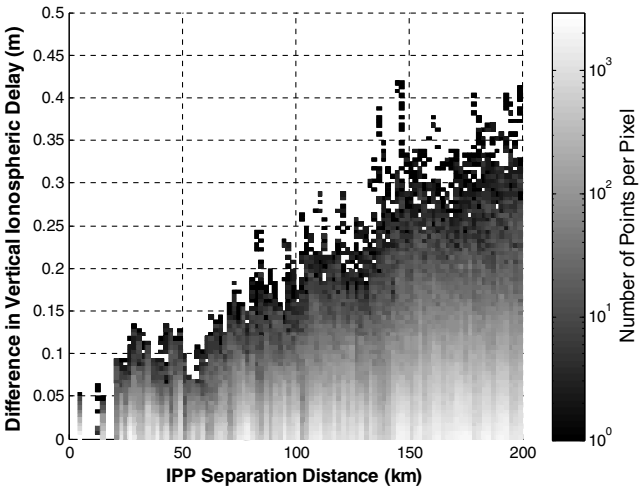

Fig. 8 Differential vertical ionosphere delay results on a quiet day (2 July 2000) from the station-pair method and JPL–CORS data (with noise reduction and bias removal).

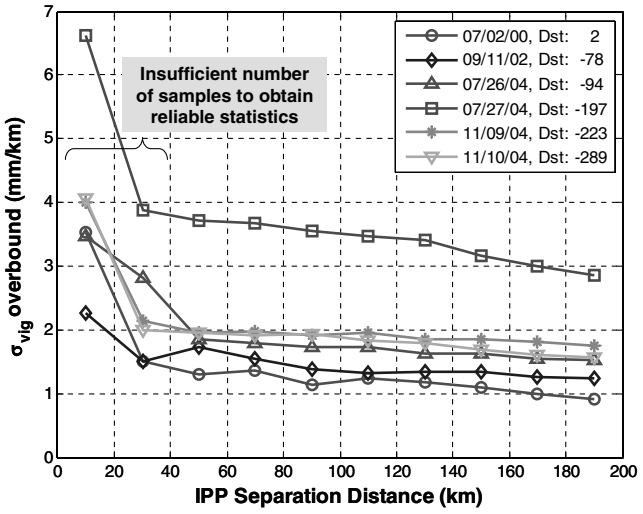

Fig. 10 σ_{vig} overbound results from the station-pair method and JPL–CORS data for all six days (with noise reduction and bias removal).

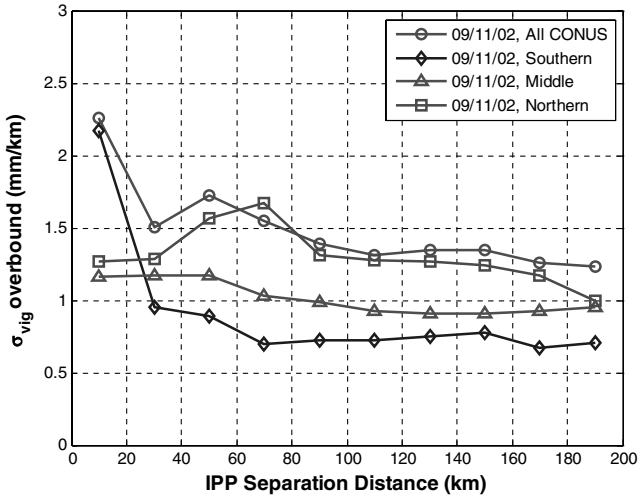

Fig. 11 σ_{vig} overbound results of all subregions from the station-pair method and JPL–CORS data for a moderate day (11 September 2002).

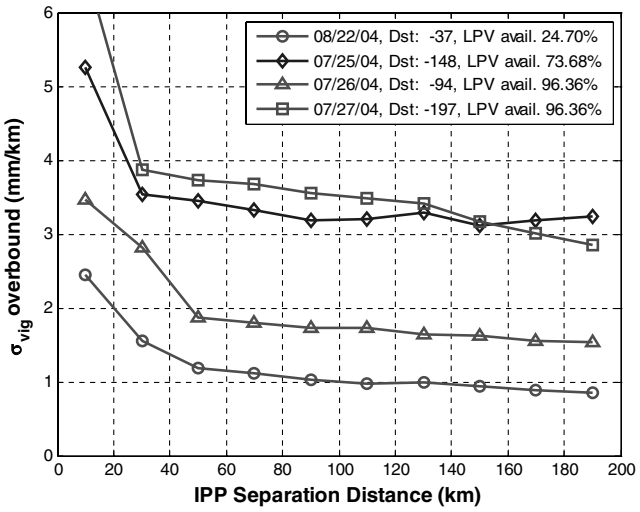

Fig. 12 σ_{vig} overbound results of WAAS-affected days from the station-pair method and JPL–CORS data.

the region of short separation distances. Therefore, this result supports the fact that σ_{vig} is conservatively bounded by 4 mm/km on nominal days.

VI. Sensitivity Analysis

This section addresses some concerns about whether the σ_{vig} of 4 mm/km is truly sufficient enough to cover ionosphere spatial decorrelation in CONUS for nominal days. First of all, because the southern sites are closer to the geomagnetic equator, those stations may not be covered by the number derived from all CONUS stations combined. The geographic trend of ionospheric gradients is thus examined in Sec. VI.A. The second analysis checks whether GBAS can operate "nominally" as well on days in which WAAS LPV availability was affected by ionosphere storms (or possibly nonionosphere events such as a loss of signals in space) but which were not severe enough to be threatening to GBAS users. Section VI.B discusses σ_{vig} dependency on WAAS availability.

A. Geographic Trend

To investigate geographic trends, the CONUS stations were subdivided into three groups: "northern" for latitudes of 40–50°, "central" for latitudes of 33–40°, and "southern" for latitudes of 23–33°. The data from those subregions were then used to compute statistics for each region separately. Figure 11 shows the estimates of σ_{vig} for a "moderate" day (11 September 2002). The estimates of each group were derived using the station-pair method and bias-removed JPL–CORS data, and were compared to the σ_{vig} estimated with all CONUS stations. On this moderate day and other days examined, no significant geographic trend was observed. In fact, by dividing CONUS into subregions, we were able to reduce the inflation factor (from 2.5 to about 1.8) which may have been increased additionally due to the mixing of non-Gaussian distributions of ionospheric gradients from all three regions.

B. Dependency on WAAS LPV Availability Coverage

Two more days (bold in Table 1) in which WAAS LPV coverage was poor (24.70 and 73.68%, respectively) were examined. The σ_{vig} estimates of those two days (the curves with circles and diamonds) are compared to those of days with nominal WAAS coverage (greater than 95%) in Fig. 12. The σ_{vig} overbounds of the days with poor WAAS coverage are still bounded by 4 mm/km. The relatively flat lines shown at longer separation distances can be extended for the estimates at IPP distances less than 40 km, by applying the same logic (the effect of the remaining biases are amplified at short separation distances and greatly degrade the accuracy of σ_{vig} estimates) explained in Sec. V.B. Therefore σ_{vig} of 4 mm/km does not need to be changed to cover any nonstormy WAAS-affected days.

VII. Conclusions

This study has demonstrated with both the WAAS supertruth data and postprocessed CORS data that, while typical ionosphere spatial decorrelation in CONUS is approximately 1 mm/km at a one-sigma level, a significantly higher value should be broadcast for σ_{vig} by GBAS stations to bound active (but not stormy) ionospheric conditions as well as quiet conditions. The results in this paper suggest that σ_{vig} of 4 mm/km is sufficient to cover almost all ionospheric conditions in CONUS. However, a precise assessment of the bounding value of σ_{vig} cannot be made from postprocessed WAAS and CORS data because of the relatively large baselines between WAAS and CORS reference stations (compared to typical LAAS reference-to-user baselines) and because $L1$–$L2$ interfrequency biases cannot be completely removed from this data.

Once several GBAS sites are fielded in different parts of CONUS, additional analysis should be done on the apparent ionospheric spatial gradients between GBAS reference-station antennas or, better yet, between the reference point and a fixed "pseudouser" antenna several kilometers away. A combination of single-frequency code-minus-carrier data and $L1$–$L2$ data with carefully calibrated interfrequency biases could help in reducing the conservatism that we believe is present in the 4 mm/km one-sigma bound. Absent additional data, 4 mm/km appears sufficient to cover all nonanomaly ionospheric conditions in CONUS with an adequate safety margin.

Acknowledgments

Funding support from the Federal Aviation Administration (FAA) Satellite Navigation Program Office is acknowledged. The authors would like to thank Todd Walter, Jason Rife, Ming Luo, and Juan Blanch of Stanford, Boris Pervan and Livio Gratton of the Illinois Institute of Technology (IIT), and John Warburton of the FAA Technical Center for their help during this research. We also would like to express special thanks to Attila Komjathy at the Jet Propulsion Laboratory (JPL) for providing us with data and comments. The advice and interest of many other people in the Stanford Global Positioning System (GPS) research group are appreciated.

References

[1] "Minimum Operational Performance Standards for GPS/Local Area Augmentation System Airborne Equipment," RTCA, Rept. SC-159 WG-4A, DO-253A, Washington, D.C, Nov. 2001.

[2] Kolb, P. F., Chen, X., and Vollath, U., "A New Method to Model the Ionosphere Across Local Area Networks," *Proceedings of the Institute of Navigation GNSS 2005*, Inst. of Navigation, Alexandria, VA, 2005, pp. 705–711.

[3] Datta-Barua, S., Walter, T., Pullen, S., Luo, M., Blanch, J., and Enge, P., "Using WAAS Ionospheric Data to Estimate LAAS Short Baseline Gradients," *Proceedings of the Institute of Navigation National Technical Meeting*, Inst. of Navigation, Alexandria, VA, 2002, pp. 523–530.

[4] "Specification: Performance Type One Local Area Augmentation System Ground Facility", U.S. Federal Aviation Administration, FAA-E-2937A, Washington, D.C, April 2002.

[5] Luo, M., Pullen, S., Datta-Barua, S., Zhang, G., Walter, T., and Enge, P., "LAAS Study of Slow-Moving Ionosphere Anomalies and Their Potential Impacts," *Proceedings of the Institute of Navigation GNSS 2005*, Inst. of Navigation, Alexandria, VA, 2005, pp. 2337–2349.

[6] Klobuchar, J., "Ionospheric Effects on GPS," *Global Positioning System: Theory and Applications*, edited by B. W. Parkinson and J. J. Spilker, Vol. 1, Progress in Astronautics and Aeronautics, AIAA, Washington, D.C., 1996, pp. 485–515.

[7] "GNSS Based Precision Approach Local Area Augmentation System (LAAS) Signal-in-Space Interface Control Document (ICD)," RTCA, Rept. SC-159 WG-4A, DO-246C, Washington, D.C., April 2005.

[8] Wilson, B. D., and Mannucci, A. J., "Instrumental Biases in Ionospheric Measurements Derived from GPS Data," *Proceedings of the Institute of Navigation GPS 1993*, Inst. of Navigation, Alexandria, VA, 1993, pp. 1343–1351.

[9] Komjathy, A., Sparks, L., and Mannucci, A. J., "A New Algorithm for Generating High Precision Ionospheric Ground-Truth Measurements for FAA's Wide Area Augmentation System," JPL Supertruth Document, Vol. 1, Jet Propulsion Laboratory, Pasadena, CA, July 2004.

[10] Komjathy, A., Sparks, L., and Mannucci, A. J., "The Ionospheric Impact of the October 2003 Storm Event on WAAS," *Proceedings of the Institute of Navigation GNSS 2004*, Inst. of Navigation, Alexandria, VA, 2004, pp. 1298–1307.